THE RARE KAON DECAY PROGRAM AT BROOKHAVEN

Maged S. Atiya

Physics Department
Brookhaven National Laboratory
Upton, New York 11973

ABSTRACT

The current status and results from the Brookhaven rare kaon decay program are presented. The anticipated upgrades and the ultimate objectives of the current programs are also discussed.

1. Introduction

The interest in rare kaon decays displayed during the last decade has been motivated by the desire to pursue both new phenomena and the detailed verification of the Standard Model. Technological advances in detector technology also make it possible to pursue these decays at the levels necessary. The current round of rare kaon experiments is sufficiently mature to allow a summary of the results of the various experiments and prediction about the likely branching ratio sensitivities to be explored by the future upgrades.

2. Description of Experiments

The past decade has seen four major detectors exploring the various decay modes of both neutral and charged kaons. These detectors are:

Experiments	Decay Particle	Primary Modes
E780/845	K_L	$K_L^0 \to \mu^\pm e^\mp$ $K_L^0 \to \mu^+\mu^-$ $K_L^0 \to e^+e^-$ $K_L^0 \to \pi^0 e^+e^-$ $K_L^0 \to \gamma e^+e^-$ $K_L^0 \to e^+e^-\gamma\gamma$ $K_L^0 \to e^+e^-e^+e^-$
E791/871	K_L	$K_L^0 \to \mu^\pm e^\mp$ $K_L^0 \to e^+e^-$ $K_L^0 \to \mu^+\mu^-$
E777/E851/E865	K^+ (in flight)	$K^+ \to \pi^+\mu^+e^-$ $K^+ \to \pi^+e^+e^-$ $\pi^0 \to e^+e^-$
E787	K^+ (stopping)	$K^+ \to \pi^+\nu\bar{\nu}$ $K^+ \to \pi^+\mu^+\mu^-$ $\pi^0 \to \nu\bar{\nu}$ $K^+ \to \pi^+\gamma\gamma$

Each of the above experiments is described below. In all cases, except E780/845, the experimenters are in the process of upgrading their detector to handle the higher AGS rates anticipated with the advent of the booster and to further suppress any backgrounds.

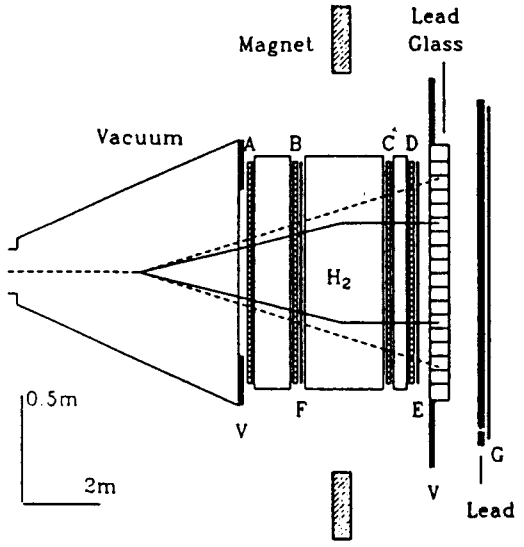

Figure 2.1: The apparatus of Experiment E845.

2.1. E780/845

Figure 2.1 shows the apparatus of E780/845, which is a collaboration of BNL and Yale University[1]. The detector is optimized for the detection of K_L^0 decays with γ and $e^\pm$ in final states. In fact, E845 originated as a dedicated $K_L^0 \to e^+e^-$ experiment. The experiment has a single magnet for momentum analysis, a hydrogen Cerenkov counter for particle identification, a lead glass array for electron measurement and a drift chamber spectrometer. The emphasis on electrons and photons in this detector expanded the reach of the experiment beyond $K_L^0 \to e^+e^-$ to other decays such as $K_L^0 \to \pi^0 e^+e^-$, $K_L^0 \to \gamma e^+e^-$ $K_L^0 \to e^+e^-\gamma\gamma$ and $K_L^0 \to e^+e^-e^+e^-$.

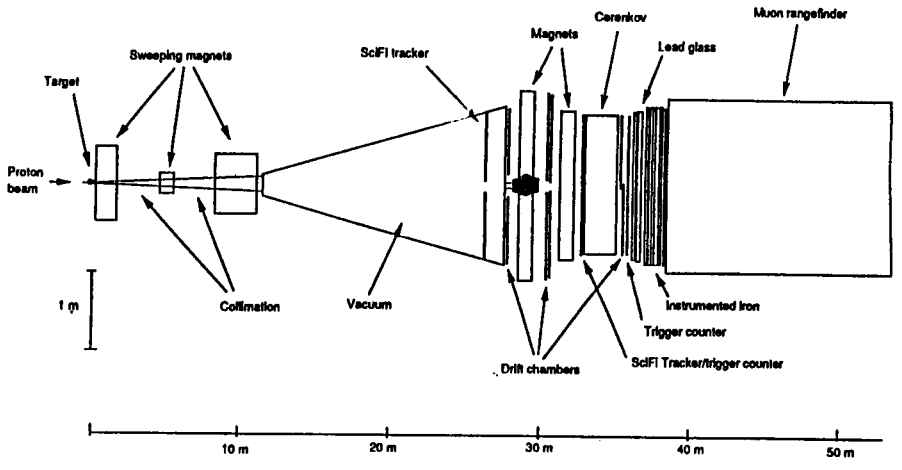

Figure 2.2: Experiment 791 apparatus.

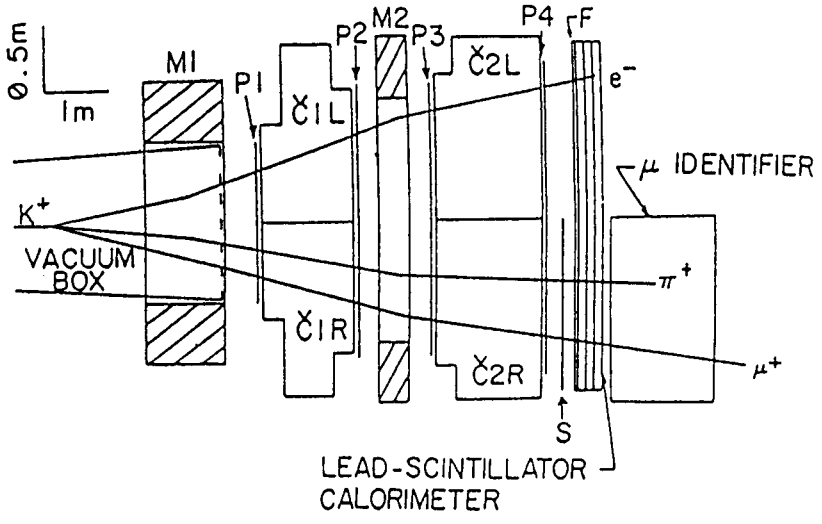

Figure 2.3: Experiment 777 apparatus.

2.2. E791/871

This experiment is optimized for the detection of two-body decays of the K_L^0 meson. The kaons are generated from a charged proton beam. Sweeping magnets remove most of the charged particles in the beam. The neutral kaon decays occur in an 8 meter vacuum tank. The detector, shown in Fig. 2.2, is a high resolution forward spectrometer. This experiment aims at achieving the best possible two-particle mass resolution through the use of two equal kick (300 MeV/c) double magnets. It also aims at achieving clean identification of electrons and muons. The former is achieved through the use of a 13.8 radiation length lead glass array and a Cerenkov counter. The latter is achieved through the use of 91 cm iron wall and scintillation hodoscopes, with a marble/proportional tube range finder. A novel aspect of the experiment is the high bandwidth data acquisition system coupled with a high rate capability (about 4 MHz for double particle rate) for the drift chambers. The upgraded experiment (E871) has an additional beam plug to allow an increase in the kaon decay rate without a corresponding increase in the singles rate at the drift chambers.

2.3. E777/851/865

This experiment is optimized for three-body in-flight decays of the K^+ meson. Figure 2.3 shows the detector used for both E777 and E851[2]. The incident beam is a 5.8 GeV unseparated beam, with the decays observed in flight. A flux of about 10^7 kaons per one second spill (with 20 times as many pions and protons) decayed in a 5 m long vacuum box. About 10% of the incident kaons decayed in the vacuum box; the remainder passed through the deadened central region of the detector. Charged particles were bent twice in opposite directions in the two dipole magnets M1 and M2. The first bend served to direct oppositely charged particles to two distinct sides of the detector; the second dipole and four stations of proportional wire chambers were used to measure the momentum of charged tracks. The momentum resolution of the spectrometer (in GeV/c) was $\sigma_p = 0.01p^2$ from 0.6 to 4.0 GeV/c.

The detector was designed with one half optimized for electron detection, and the other half for pion or muon detection. Electrons were identified by a positive signal in the two hydrogen threshold Cerenkov counters and a large energy deposition in a lead-scintillator shower counter. On the other half of the detector, two Cerenkov counters filled with CO_2 had a threshold near the cutoff

of the muon spectrum from $K^+ \to \pi^+\mu^+e^-$ at 3.7 GeV/c. The logical OR of these two counters is used to reject positrons with a 99.9% efficiency. Behind the shower counter was a muon detector made from steel plates and proportional tubes.

The trigger for $K^+ \to \pi^+\mu^+e^-$ initially required three charged tracks as measured with scintillation counter hodoscopes and a potential muon track in the muon detector and an electron candidate in the hydrogen Cerenkov counters. About 250 such events per spill were read into 68020 microprocessors (FERMILAB ACP nodes) which were programmed to find three acceptable tracks with a distance of closest approach to a common vertex of less than 10 cm (about 10 sigma), rejecting 95% of the triggers. About 3×10^7 events were written on tape for analysis offline.

The upgrade to E777/851 is the future E865. Figure 2.4 shows the new apparatus of E865. The factor of 70 increase in acceptance over E777 is achieved by a seven fold improvement in beam intensity per incident proton due to the construction of a new beam, and a factor 10 improvements in the acceptance. The latter is achieved by a combination of larger aperture, improved trigger efficiency, the identification of both lepton charges and longer running time. E865 is due to start taking data in 1994-1995.

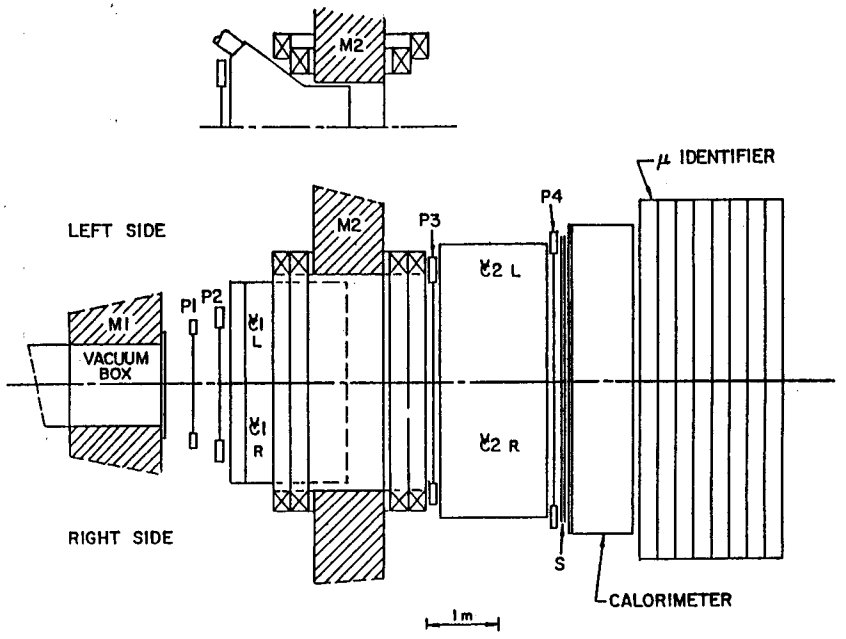

Figure 2.4: Experiment 865 apparatus.

2.4. E787

This experiment is optimized for the decay $K^+ \to \pi^+\nu\bar{\nu}$. To assist with kinematic reduction of backgrounds, the decay is observed at rest using a stopping kaon beam. The detector[3] is shown in Fig. 2.5. A kaon beam of 800 MeV/c momentum is incident from the left. Typical beam intensities range between 1 and 1.5 million kaons, with an equal number of protons and twice as many pions. The beam is analyzed in a set of beam counters. The beam is then slowed by a degrader to about 300 MeV/c momentum. The degrader is made of BeO with the last section made of lead glass to assist in photon identification.

The slowed kaons decay in a target made of 2269 2 mm scintillating fibers, read out by 384 1 cm phototubes. An end view of the target is shown in Fig. 2.6, with a kaon decay into one charge track (in this case a pion). The live target serves many purposes: the clean identification of tracks to correct for energy and momentum loss, the rejection of in-flight decay by imposing a 2 nsec interval cut between the entry of the kaon and the appearance of the charged products, and the identification of photons converting in the target.

The decay products are analyzed in a thin circular drift chamber in the presence of a 1 Tesla solenoidal field. The momentum resolution of 2.5% for a 200 MeV/c track was limited by multiple scattering in the chamber.

Charged tracks exiting chambers were slowed, and in most cases stopped, in a pure scintillator calorimeter with two layers of drift chambers. The calorimeter, called the range stack, measures the range, energy, and the species of the particle through identification of its decay products. The range stack is segmented into 24 azimuthal sectors and 21 radial sections, the first ten of which ganged in four, three and two radial layers.

The measurement of the particle species is made by a system of 300 500 MHz sampling, 8-bit waveform digitizers[4]. These devices create an electronic image in both time and space for each charged track for each counter. Figure 2.7 shows an example of such a measurement. The vertical columns show the view from both upstream and downstream ends of the calorimeter. The horizontal rows show the view from each counter in depth. It is clear that an incident pion is stopped in the second row, decays into a muon, which in turn decays into an electron.

The entire detector is surrounded by a hermetic lead-scintillator counter to observe both direct photons and π^0 decay photons. The π^0 rejection probability is close to 10^{-6}, with the veto deadtime kept to under 20%

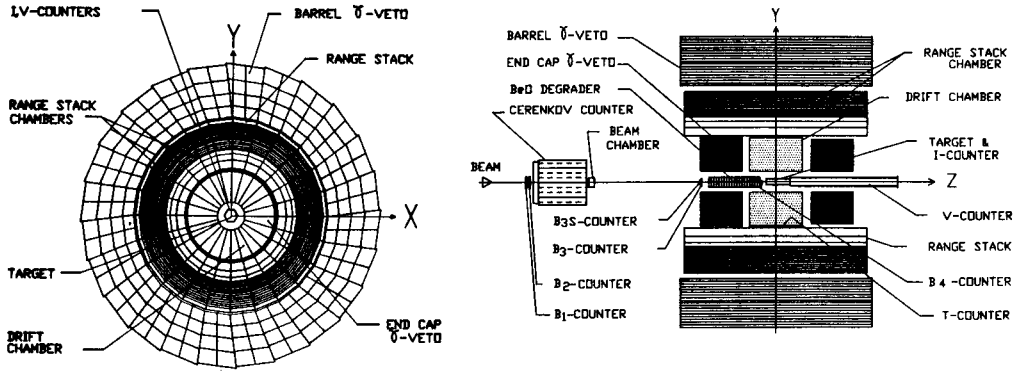

Figure 2.5: Experiment 787 apparatus.

during normal running conditions. This is achieved by setting a threshold of 1 MeV of visible energy and a time gate of 1 nsec using the waveform digitizers.

Experiment E787 is undergoing a major upgrade designed to ready the experiment for the next phase. The upgrades include the introduction of a crystal photon veto to improve the veto efficiency and lower the deadtime. They also include an improved drift chamber and range stack for better momentum, range and energy measurements. The entire data acquisition and trigger system are being rebuilt to allow high intensity running. The fiber target has been upgraded to improve the light yield. The *new* E787 will be running in late 1993.

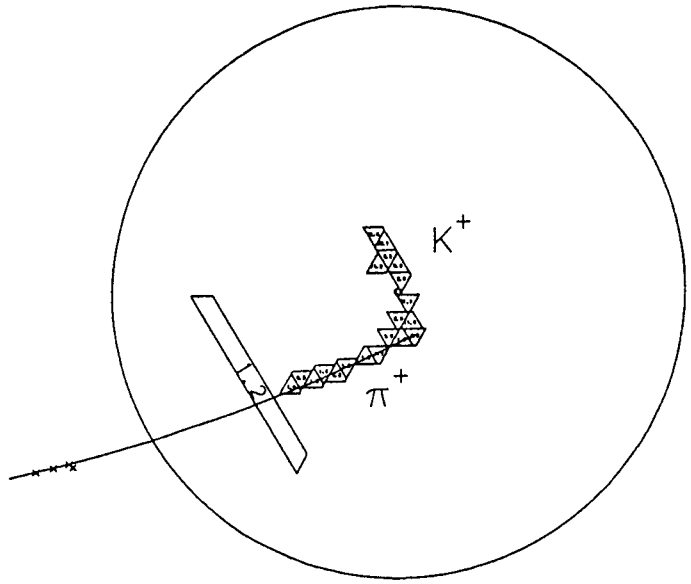

Figure 2.6: End view of E787 target showing kaon decay into a single charged pion and neutral products, probably π^0.

3. Physics Signals

Next we discuss the status of each of the decay modes examined by the above experiments. We emphasize both the current physics picture and future potential.

3.1. $K_L^0 \to \mu^\pm e^\mp$

This decay is forbidden in the Standard Model as it violates lepton flavor conservation. The experiment is sensitive to predictions made by various extensions to the Standard Model. Should the decay be mediated by a horizontal gauge boson, **H**, then the branching ratio is predicted to be[5]

$$B\left(K_L^0 \to \mu^\pm e^\mp\right) = B\left(K^+ \to \mu^+ \nu\right) \times \frac{\tau_L}{\tau_+} \times \left(\frac{M_W}{M_H}\right)^4 .$$

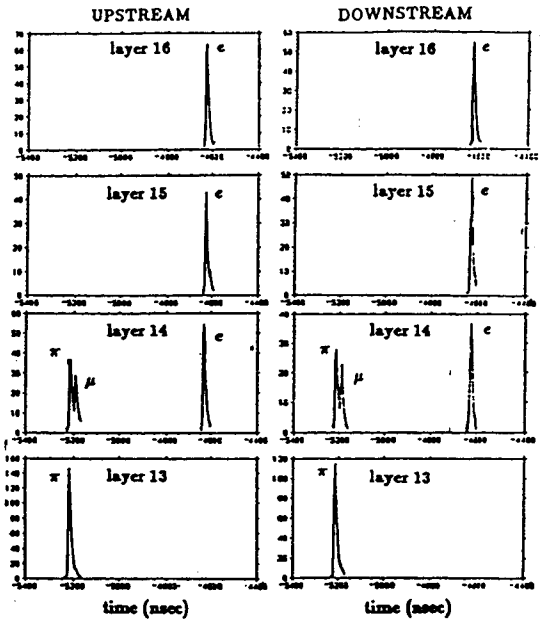

Figure 2.7: Example of particle identification by waveform digitizers, see text for explanation.

The current limit given by E791[6,7] is $\leq 3.3 \times 10^{-11}$ leading to a mass of 110 TeV for the **H** boson, and assuming the same coupling as the W. This is a scale well beyond the highest hadron colliders existing or planned. Hence the $K_L^0 \to \mu^{\pm} e^{\mp}$ decay represents a unique laboratory for studying lepton flavor violation. The new E791 should approach the level of 10^{-12} for this decay, thus further expanding the mass region for **H**, or possibly finding the decay.

The branching ratio obtained by E791 is impressive in view of both the rates necessary for this observation and the backgrounds present at that level. The experiment ran in a mode where the two particle rates in the drift chambers exceeded 1 MHz [8], yet sufficient resolution is maintained to reject the backgrounds. The primary background in E791 was the $K_L^0 \to \pi^{\pm} e^{\mp} \nu$ decay. The probability of misidentifying a pion as a muon was about 10%. This represents a serious challenge at the trigger level, which was overcome by the sophisticated trigger processing electronics. However, the background also persists at the analysis level where the pion is misidentified as an electron, and the electron is misidentified as a muon. This double misidentification is particulary serious as it will generate masses at or above the kaon mass. The background is overcome by a combination of good particle identification and

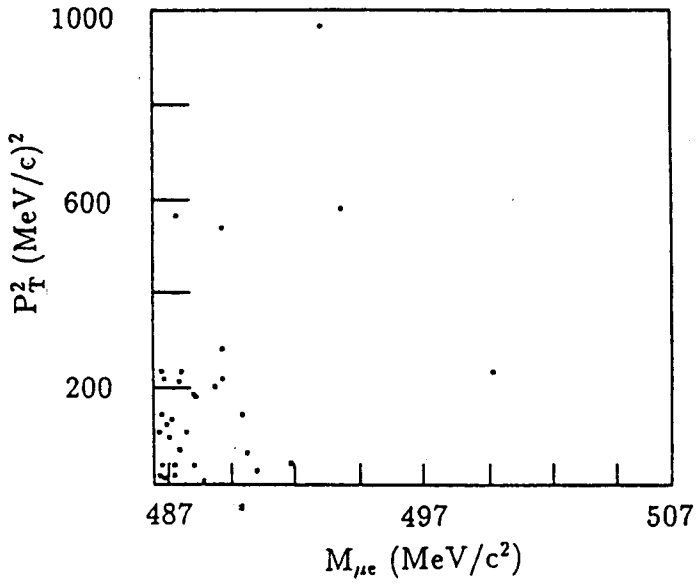

Figure 3.1: The $\mu - e$ pair effective mass vs. ${P_T}^2$ from E791.

good mass resolution. Figure 3.1 shows the $\mu - e$ pair effective mass resolution vs. ${P_T}^2$ from a single data run (1990)[7]. The combined analysis of three data runs yields the $\leq 3.3 \times 10^{-11}$ branching ratio limit quoted earlier.

3.2. $K^+ \to \pi^+ \mu^+ e^-$

The decay $K^+ \to \pi^+ \mu^+ e^-$ is the charged counterpart to the $K_L^0 \to \mu^{\pm} e^{\mp}$. The less favorable phase space renders it somewhat less sensitive than the $K_L^0 \to \mu^{\pm} e^{\mp}$ to all lepton flavor violating decays, except those due to a purely vector interaction.

The $K^+ \to \pi^+ \mu^+ e^-$ branching ratio was measured to be $\leq 2.1 \times 10^{-10}$ by E777 [9]. Also the decay $B(\pi^0 \to \mu^+ e^-)$ was measured to be $\leq 1.6 \times 10^{-8}$ by the same experiment. The leading background to these decays are misidentification of decay particles in any of the three decays $K^+ \to \pi^+ \pi^+ \pi^-$ or $K^+ \to \pi^+ \pi^0$; $\pi^0 \to e^+ e^- \gamma$. The experimenters were able to suppress these backgrounds by a careful effort in the Cerenkov counters and lead-scintillator calorimeter. Figure 3.2 shows the distribution of the three-body invariant mass plotted against the "vertex miss" distance for both the clearly identified $K^+ \to$

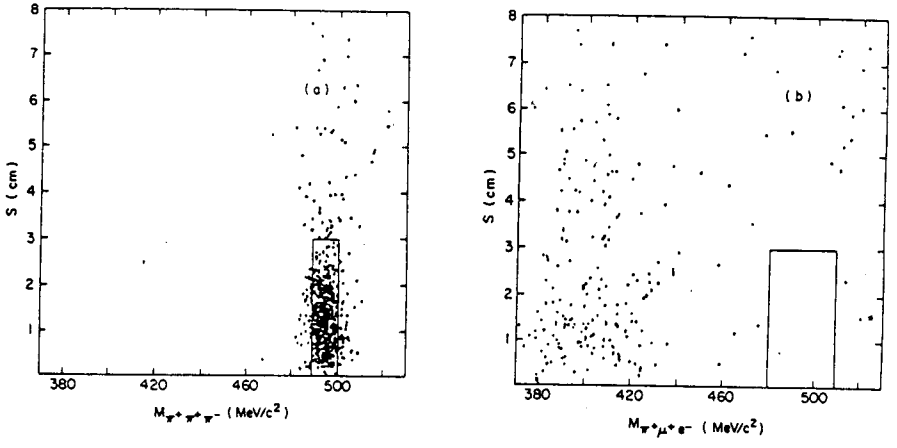

Figure 3.2: The vertex miss distance S vs. invariant mass for (a) $K^+ \to \pi^+\pi^+\pi^-$ and (b) $K^+ \to \pi^+\mu^+e^-$ candidates in E777.

$\pi^+\pi^+\pi^-$ and the presumed $K^+ \to \pi^+\mu^+e^-$ events. The vertex miss distance should be zero for events from the center of the kaon beam, and hence expresses both the quality of the fit and the size of the beam. The search region is bigger in $K^+ \to \pi^+\mu^+e^-$ than $K^+ \to \pi^+\pi^+\pi^-$ due to the larger Q value.

3.3. $K^+ \to \pi^+\nu\bar{\nu}$

The decay $K^+ \to \pi^+\nu\bar{\nu}$ is a second order suppressed decay with negligible long distance corrections. This makes it a useful probe of the CKM matrix and the Standard Model parameter, and a fertile ground for observation of any effects beyond the Standard Model. This feature has been widely recognized, and contributes to the desire to observe this decay down to the Standard Model level. The Standard Model prediction of $K^+ \to \pi^+\nu\bar{\nu}$ is calculated by various authors with loops involving heavy charge 2/3 quarks, as shown in the Feynman diagrams in Fig. 3.3.

The branching ratio for $K^+ \to \pi^+\nu\bar{\nu}$ is given in the Standard Model for three light neutrino types as[10,11]

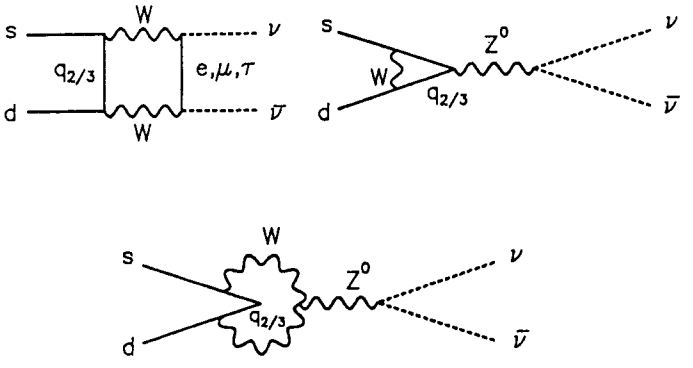

Figure 3.3: Feynman diagrams which contribute to the decay $K^+ \to \pi^+\nu\bar{\nu}$ in the Standard Model.

$$B_{K^+\to\pi^+\nu\bar{\nu}} = \frac{3\alpha^2 B_{K^+\to\pi^0 e^+\nu}}{8\pi^2 \sin^4\theta_W} \frac{|\, V_{cs}^* V_{cd} D_c + V_{ts}^* V_{td} D_t \,|^2}{|\, V_{us} \,|^2} ,$$

where the CKM matrix[12] is expressed as

$$\begin{pmatrix} V_{ud} V_{us} V_{ub} \\ V_{cd} V_{cs} V_{cb} \\ V_{td} V_{ts} V_{tb} \end{pmatrix} .$$

Wolfenstein[13] has expressed the CKM matrix in the following parameterization in powers of the Cabibbo angle, λ:

$$\begin{pmatrix} 1-\lambda^2/2 & \lambda & A\lambda^3(\rho - i\eta) \\ -\lambda & 1-\lambda^2/2 & A\lambda^2 \\ A\lambda^3(1-\rho-i\eta) & -A\lambda^2 & 1 \end{pmatrix}$$

where the CP violating phase is represented by the (ρ, η) point in the complex plane.

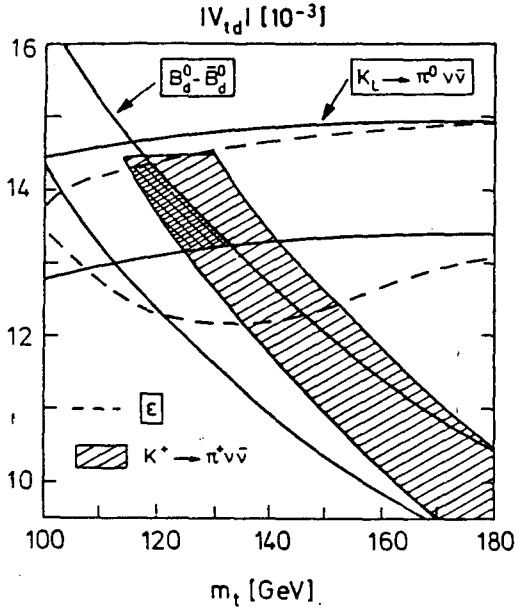

Figure 3.4: The $|V_{td}|$ vs m_t for a $K^+ \to \pi^+\nu\bar{\nu}$ branching ratio of 10^{-10} and the three shown values of $|V_{cb}|$.

In the Wolfenstein parameterization of the CKM matrix, the decay can then be represented[14] as

$$\frac{B_{K^+\to\pi^+\nu\bar{\nu}}}{B_{K^+\to\pi^0 e^+\nu}} \cdot \frac{8\pi^2 \sin^4\theta_W}{3\alpha^2} \cdot \frac{1}{A^4\lambda^8 D_t^2} = \eta^2 + \left(1 + \frac{(1-\lambda^2/2)}{A^2\lambda^4}\frac{D_c}{D_t} - \rho\right)^2 .$$

Thus, a measurement of $K^+ \to \pi^+\nu\bar{\nu}$ determines a circle in the $\rho-\eta$ plane. This observation has been made recently by several authors[14,15] and used to constrain the mass of the top quark and $|V_{td}|$. Other authors[16] have also pointed out, and been troubled by, the strong dependence on the mass of the top quark. However, an analysis by Buras and Harlander[15] has shown that the decay remains the cleanest means of measuring $|V_{td}|$, once the mass of the top quark is known. Figure 3.4[15] shows the region of $|V_{td}|$ and m_t for a $K^+ \to \pi^+\nu\bar{\nu}$ branching ratio of 10^{-10}, assuming the current accepted values for the $\frac{|V_{ub}|}{|V_{cb}|}$ and three values of $|V_{cb}|$ of .046, .041 and .036.

The experimental situation is rather promising. The latest result[17] from E787 shows a branching ratio limit of

$$B\left(K^+ \to \pi^+\nu\bar{\nu}\right) \leq 5 \times 10^{-9}$$

which is less than a factor of 50 away from the most pessimistic Standard Model predictions.

The study of the $K^+ \to \pi^+\nu\bar{\nu}$ remains a difficult task given the poor signature of the decay and the large backgrounds from the $K^+ \to \pi^+\pi^0$ and $K^+ \to \mu^+\nu$. The initial strategy of E787 has been to confine the search to the kinematic region above the $K^+ \to \pi^+\pi^0$ pion momentum to reduce the pion contamination. Several cuts are imposed on the data: a waveform digitizer cut to reduce the muon background by a factor of over 10^{-6}, and a photon veto cut to reduce the $K^+ \to \pi^+\pi^0$ background by a factor 2×10^{-6}. The energy vs. range distribution of the data and Monte Carlo are shown in Fig. 3.5. The rectangular box describes the search area above the $K^+ \to \pi^+\pi^0$ peak. The data shows the $K^+ \to \pi^+\pi^0$ and $K^+ \to \mu^+\nu$ and no $K^+ \to \pi^+\nu\bar{\nu}$ signal in the search region. Detector upgrades should reduce these backgrounds by over an order of magnitude due to a crystal calorimeter with better photon rejection efficiency and an improved momentum and energy measurement system. These improvements, coupled with an order of magnitude improvement in beam intensity, will allow the observation of the decay $K^+ \to \pi^+\nu\bar{\nu}$ by 1997.

Recently E787 has attempted a search for $K^+ \to \pi^+\nu\bar{\nu}$ *below* the $K^+ \to \pi^+\pi^0$ peak. The preliminary results[18] from this search indicate a branching ratio limit of $\leq 1.7 \times 10^{-8}$.

3.4. $K_L^0 \to \mu^+\mu^-$

Experiment E791[19] has also measured the decay $K_L^0 \to \mu^+\mu^-$ in three different runs of increasing sensitivity, as shown in the table below.

Table 3.1: $K_L^0 \to \mu^+\mu^-$ branching ratio as measured by Experiment 791.

Year	Events	Branching ratio
1988	88	$(5.8 \pm 0.6 \pm 0.4) \times 10^{-9}$
1989	281	$(7.6 \pm 0.5 \pm 0.4) \times 10^{-9}$
1990	349	$(6.96 \pm 0.40 \pm 0.22) \times 10^{-9}$

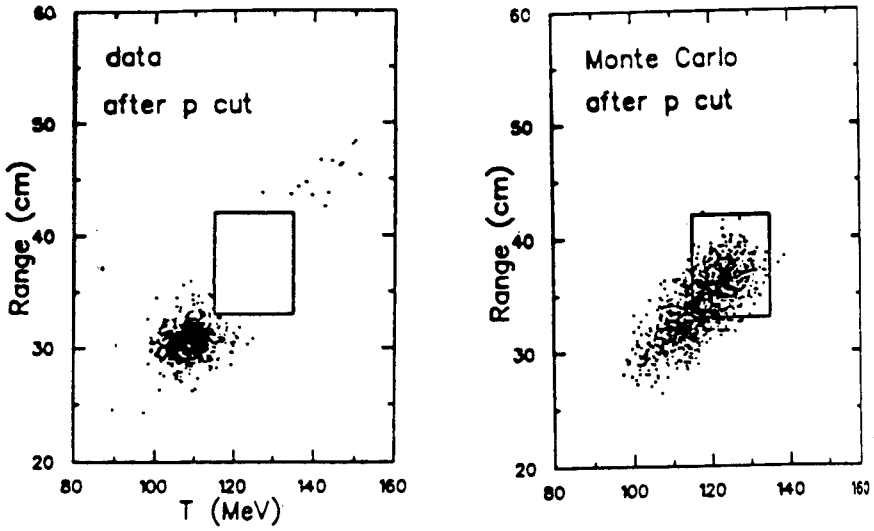

Figure 3.5: The range vs. kinetic energy of the $K^+ \to \pi^+\nu\bar{\nu}$ candidates and the Monte Carlo simulation.

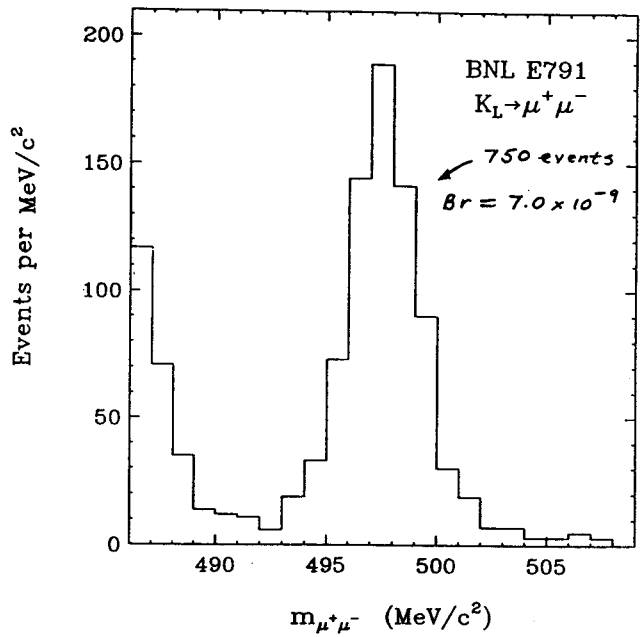

Figure 3.6: The spectrum of the decay $K_L^0 \to \mu^+\mu^-$ as seen in E791.

The experimental signal is clean as shown in Fig. 3.6, and displays the characteristic two-body mass resolution of E791. The three results[19,20], taken together, yield a branching ratio of $(7.0 \pm 0.4) \times 10^{-9}$. This branching ratio is interestingly small in view of the physics of the $K_L^0 \to \mu^+\mu^-$.

The decay $K_L^0 \to \mu^+\mu^-$ has a real part which is due to the electroweak component shown in Fig. 3.7 and an imaginary part which is due to the two-photo component, also shown in Fig. 3.7.

The imaginary part of the $K_L^0 \to \mu^+\mu^-$ decay has been calculated as a function of the $K_L^0 \to \gamma\gamma$ branching[21], and is given as

$$B(K_L \to \mu\mu) = 1.195 \times 10^{-5} B(K_L \to \gamma\gamma) = 6.81 \times 10^{-8} \quad .$$

The short distance contribution can then be no more than $\leq 8 \times 10^{-10}$ in branching ratio. This contribution is due to the charm and top quark diagrams and can be written as

$$B_{K_L^0 \to \mu^+\mu^-} = B_{K^+ \to \mu^+\nu} \frac{\tau_{K_L^0}}{\tau_{K^+}} \frac{\alpha^2}{4\pi^2 \sin^4\theta_W} \frac{Re\,(V_{cs}^* V_{cd} C_c + V_{ts}^* V_{td} C_t)^2}{V_{us}^2},$$

or using the Wolfenstein representation one can write

$$\sqrt{\frac{B_{K_L^0 \to \mu^+\mu^-}}{B_{K^+ \to \mu^+\nu}} \frac{\tau_{K^+}}{\tau_{K_L^0}} \frac{4\pi^2 \sin^4\theta_W}{\alpha^2}} = C_c + A^2\lambda^4 C_t (1-\rho)$$

or

$$\sqrt{\frac{B_{K_L^0 \to \mu^+\mu^-}}{7.77 \times 10^{-5}}} = C_c + \mid V_{ts} \mid^2 C_t (1-\rho)$$

where C_c and C_t are the charm and top quark kinematic functions. The charged and neutral K lifetimes are taken to be 12.37 ns and 51.8 ns, respectively, and the $K^+ \to \mu^+\nu$ branching ratio is taken to be 63.51%.

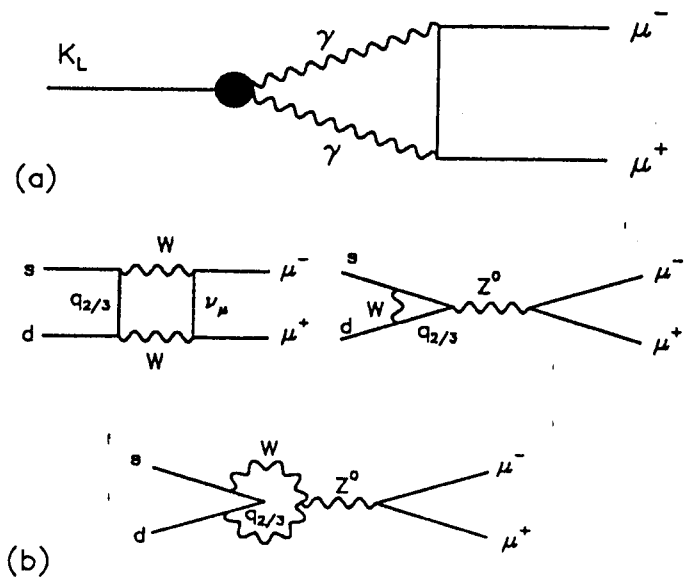

Figure 3.7: The long and short distance diagrams of the decay $K_L^0 \rightarrow \mu^+\mu^-$.

Assuming a $\mid V_{ts} \mid = 0.049$ value yields the ρ_{min} values as a function of the top quark listed in Table 3.2.

Table 3.2: Minimum values of ρ from $K_L^0 \rightarrow \mu^+\mu^-$ for various top quark masses.

m_t (GeV/c^2)	ρ_{min}
100	-0.70
125	-0.20
150	0.01
200	0.42

The small branching ratio for $K_L^0 \rightarrow \mu^+\mu^-$ implies a $K_L^0 \rightarrow e^+e^-$ branching ratio of $\leq 3 \times 10^{-12}$ which is suppressed relative to the $K_L^0 \rightarrow \mu^+\mu^-$ due to the usual helicity arguments. E791 has established a limit of $\leq 4.7 \times 10^{-11}$ on the decay, leaving an order of magnitude for either improvements, or the discovery of new physics.

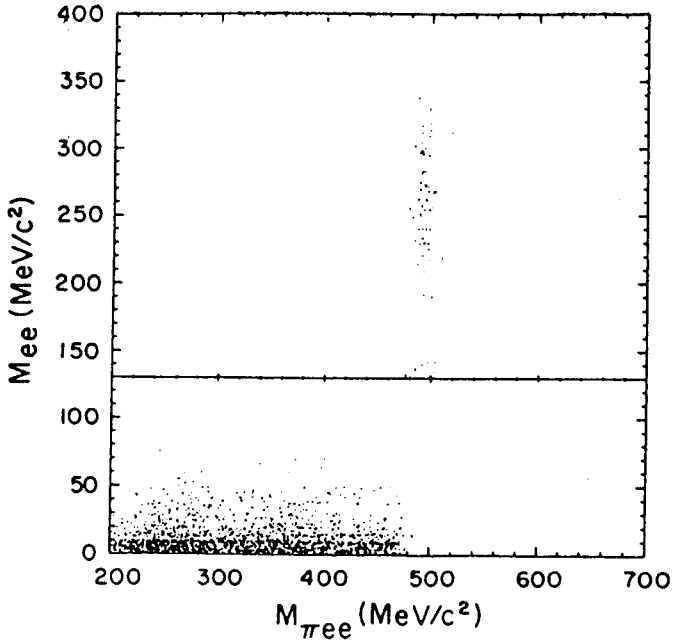

Figure 3.8: π^+ee invariant mass vs. the ee invariant mass.

3.5. $K^+ \rightarrow \pi^+e^+e^-$

The $K^+ \rightarrow \pi^+e^+e^-$ decay is an interesting example of the ability of this current round of kaon experiments to study the detailed predictions of various models [21]. The prediction of the $K^+ \rightarrow \pi^+e^+e^-$ decay was an early demonstration of the GIM suppression and the Standard Model[22]. The decay, however, was far from understood in detail[23], primarily due to long distance effects. E777/851 increased the observable sample of events by over an order of magnitude[24,25], thus allowing a more detailed study of the decay, especially the predictions of the chiral perturbation theory[23]. Figure 3.8 shows the distribution of the π^+ee invariant mass vs the ee invariant mass[26].

The region above 130 MeV in ee mass shows a clear $K^+ \rightarrow \pi^+e^+e^-$ band. The region below 130 MeV shows the background, primarily the $K_{\pi 2}$ Dalitz decay ($K^+ \rightarrow \pi^+\pi^0$, $\pi^0 \rightarrow e^+e^-\gamma$), and is, for better visibility, scaled down by 140. Figure 3.9 shows the invariant mass $M_{\pi ee}$ distribution for events with M_{ee} above 150 MeV.

The solid curve is a Monte Carlo prediction with a vector spectrum of the form

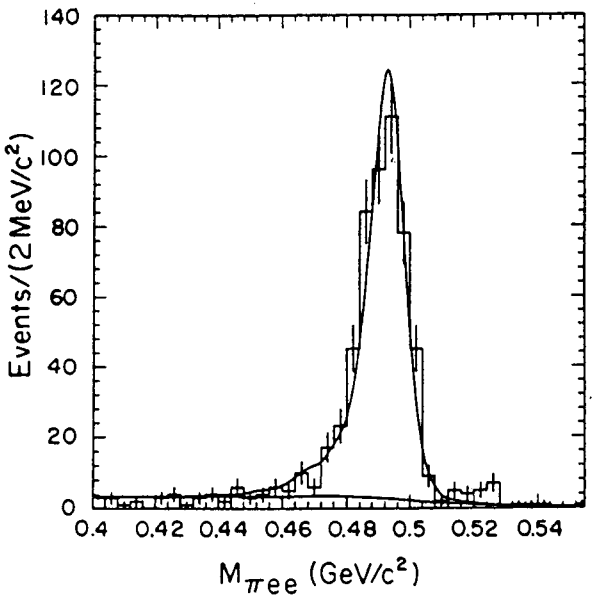

Figure 3.9: π^+ee invariant mass.

$$d\Gamma/dM_{ee} = CM_{ee}P_\pi^3\left(1+\lambda {M_{ee}}^2/{M_\pi}^2\right)^2 .$$

The overall normalization C, and λ were varied in the fit. The χ^2 contours of the fit for λ are plotted in Fig. 3.10.

Chiral perturbation theory [21] offers a means of understanding this decay. The electron pair mass spectrum is parameterized as

$$d\Gamma/dM_{ee} = 16M_{ee}\bar{\Gamma}P_\pi^3|\hat{\phi_+}|^2/m_K^5$$

where - $\hat{\phi_+} = \phi_K + \phi_\pi + w_+$ with only w_+ as a free parameter to be extracted from the data. E777/851 extracts this parameter from their measurement of the decay branching ratio and the ee pair mass. Figure 3.11 shows the measured ee pair mass and the Monte Carlo prediction for the fitted lambda value of λ=0.105. Figure 3.12 shows the allowed w_+ values with the χ^2 contours shown in Fig. 3.10.

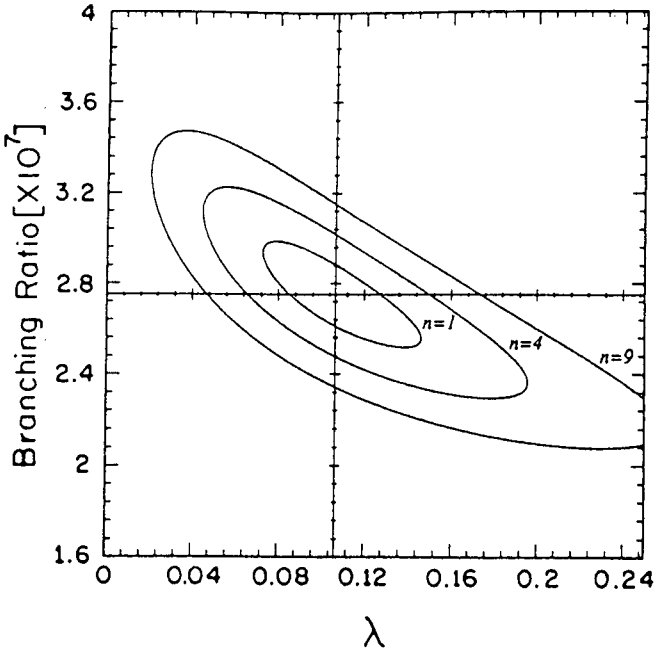

Figure 3.10: χ^2 contours for $B(K^+ \to \pi^+e^+e^-)$ vs. λ .

3.6. $\pi^0 \to e^+e^-$

The decay $\pi^0 \to e^+e^-$ has had a confused history with many conflicting observations[27,28]. Recently E777/851 has measured the decay branching ratio to be

$$B\left(\pi^0 \to e^+e^-\right) = 6.9 \pm 2.3 \pm 0.6 \times 10^{-8}$$

thus in agreement with the Standard Model predictions.

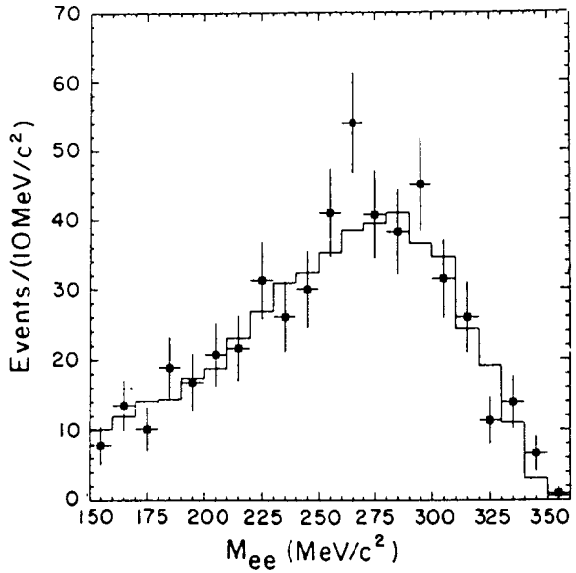

Figure 3.11: The M_{ee} spectrum for events with $470 \geq M_{\pi ee} \leq 512$ MeV. The solid curve is a Monte Carlo prediction with λ=0.105.

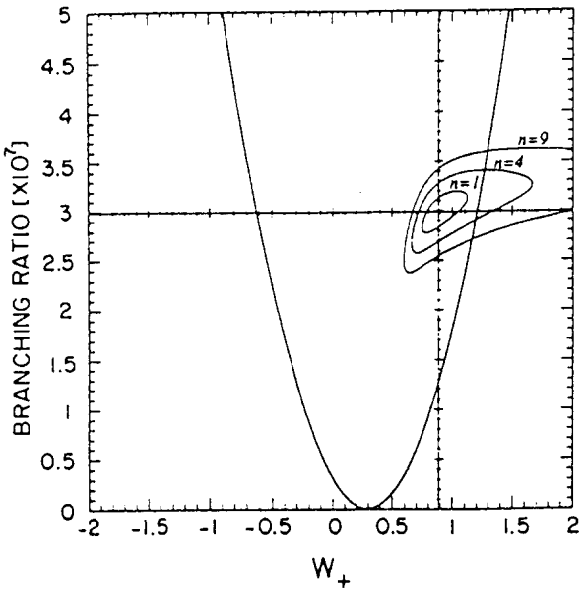

Figure 3.12: χ^2 contours vs. w^+ in the decay *pee*. The parabolic curve is a theoretical predication[23].

3.7. $K_L^0 \to \pi^0 e^+ e^-$, $K_L^0 \to \gamma e^+ e^-$, $K_L^0 \to e^+ e^- \gamma\gamma$

These three decays were studied by E845. The apparatus as mentioned earlier was optimized for the observation of photons and electrons.

$K_L^0 \to \pi^0 e^+ e^-$ has been measured[29] to be $\leq 5.5 \times 10^{-9}$. This represented a 400-fold improvement over previous searches[30], but still falls short of the 10^{-11} desired region of accuracy. The region is dictated by the direct CP-violation amplitude which is comparable in magnitude to the indirect CP-violation amplitude, allowing $K_L^0 \to \pi^0 e^+ e^-$ to be an excellent laboratory for the study of CP-violation[31,32,33]. The two orders of magnitude shortfall between the current limit and the ultimate CP-violating branching ratio will undoubtedly attract future experiments. These experiments will, however, have to contend with another result from E845.

The discovery of the decay $K_L^0 \to e^+ e^- \gamma\gamma$ at the level of $6.6 \pm 3.2 \times 10^{-7}$ is in perfect agreement with the QED calculations for $K_L^0 \to \gamma e^+ e^-$ accompanied by a hard Bremsstrahlung [34]. Unfortunately the $\gamma\gamma$ spectrum extends well beyond the π^0 mass. This means that $K_L^0 \to e^+ e^- \gamma\gamma$ is a serious background to the $K_L^0 \to \pi^0 e^+ e^-$ decay.

Another accomplishment of E845 has been an increase in the statistics of the decay $K_L^0 \to \gamma e^+ e^-$ from 4 to about 1000[35]. This allows a clean study of the form factor of the decay, $x = m_e e / {m_K}^2$. This is shown in Fig. 3.13. The dotted curve represents a ρ propagator (analogous to the η decay, while the solid curve represents a K^* propagator, which is clearly a better fit for the data. The measurement of the branching ratio yields

$$B\left(K_L^0 \to \gamma e^+ e^-\right) = 9.1 \pm 0.4^{+0.6}_{-0.5} \times 10^{-6} .$$

Additionally, E845 observed the decay $K_L^0 \to e^+ e^- e^+ e^-$ at a branching ratio of

$$B\left(K_L^0 \to e^+ e^- e^+ e^-\right) = (5 \pm 2 \pm 3) \times 10^{-8}$$

as shown in Fig. 3.14.

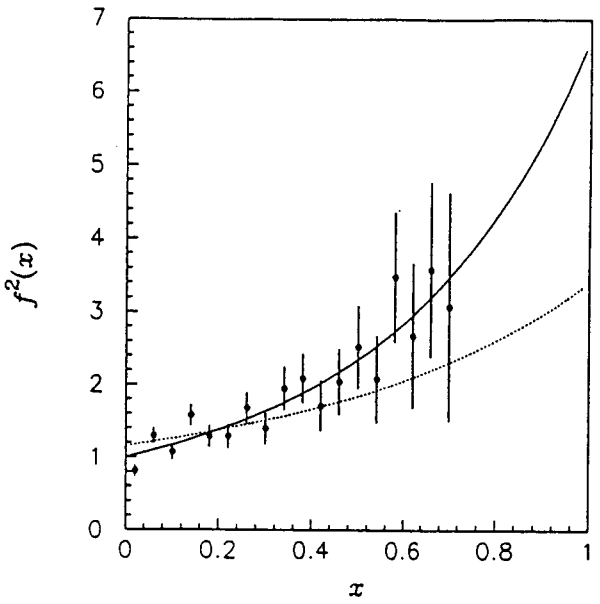

Figure 3.13: The form factor for the decay $K_L^0 \to \gamma e^+ e^-$ with a ρ propagator dotted, and a K^* propagator, solid.

3.8. Other decays from E787

The E787 detector is also suited for the observation of other kaon decays where photon identification, or rejection, plays a major role in background rejection. The E787 experiment has had considerable success in these studies, which we list here in tabular form[36,37,38].

Decay	Limit	Comments
$K^+ \to \pi^+ X^0$	$\leq 1 \times 10^{-9}$	expect 100 times improvement
$K^+ \to \pi^+ \mu^+ \mu^-$	$\leq 2.3 \times 10^{-7}$	expect observation
$K^+ \to \pi^+ \gamma\gamma$	$\leq 1 \times 10^{-6}$	expect 10 times improvement
$\pi^0 \to \nu\bar{\nu}$	$\leq 8 \times 10^{-7}$	modest improvements
$\pi^0 \to \gamma X^0$	$\leq 5.4 \times 10^{-4}$	

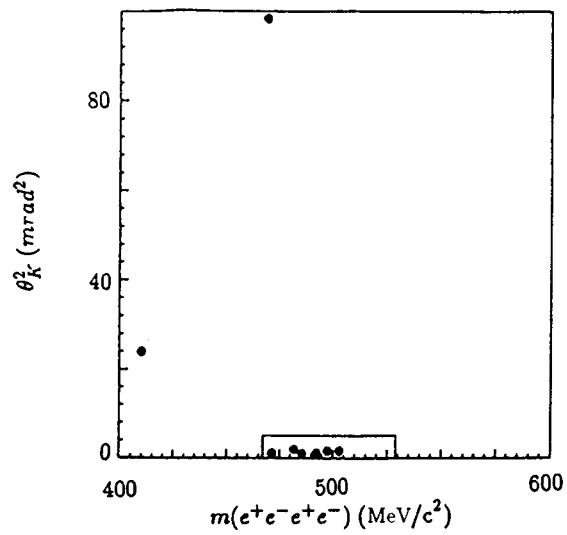

Figure 3.14: The $K_L^0 \to e^+e^-e^+e^-$ candidates mass vs. beam angle, from E845.

4. The AGS upgrades

The common feature of all the three kaon programs at Brookhaven is their need for a major increase in intensity to conclude what has been a very successful program. The AGS has responded with a program of intensity improvement with several major components.

The first component is the new AGS booster. This is a high intensity 202 m circumference synchrotron designed to improve the AGS intensity by a factor of four, as well as provide heavy ion injection to the Relativistic Heavy Ion Collider (RHIC). The booster has been completed and is currently being commissioned.

An additional component is the improvement of the AGS RF systems to allow a higher peak operating intensity. The project is currently under way, with completion slated for late 1993.

Individual experiments have also sought to improve the available intensity by rebuilding their beam lines. A newly commissioned beam line for

E787 improves the beam intensity by a factor of two per incident proton, while it lowers the pion contamination by a factor of three. The beam utilitizes a double separator and improved optics.

E865, the successor to E777, has also designed a new unseparated K^+ beam with a 6 GeV/c momentum. The new beam will use better optics and collimation to allow a factor of seven increase in the intensity, while keeping the overall rate at the detector comparable to that of E777.

5. Conclusion

The accomplishments of the rare kaon program at Brookhaven are clear. The current round of experimental upgrades coupled to the AGS intensity upgrades and the new beam lines should allow a successful completion of the current round of experiments. This will include the observation of the decay $K^+ \rightarrow \pi^+\nu\bar{\nu}$ at the Standard Model level, and either the observation of lepton flavor violating decays, or the setting of limits at the 10^{-12} level. In addition, the current program of studying the details of the Standard Model and kaon decays will be carried to new levels of precision.

6. Acknowledgments

I would like to thank my colleagues J. Haggerty, L. Littenberg, A. Schwartz and M. Zeller for many fruitfull discussions as well as the use of their data.

References

1. R.K. Adair et al., "A Search for the Rare Decay $K^0 \rightarrow \pi^0 e^+ e^-$" BNL, Yale, Vassar proposal, Jan 1988.

2. N.J. Baker et al., Phys. Rev. Lett. 59, 2832 (1987).

3. M. Atiya et al., Nucl. Instr. Meth. A321, 129 (1992).

4. M. Atiya et al., Nucl. Instr. Meth. A279, 180 (1989).

5. R.N. Cahn and H. Harari, Nucl. Phys. B176, 135 (1980).

6. C. Mathiazhagan et al., Phys. Rev. Lett. 63, 2181 (1989).

7. S. Kettell, *Proceedings of the 1991 DPF Conference*, p. 555.

8. S. Kettel, Private communication.

9. A.M. Lee et al., Phys. Rev. Lett. 64, 165 (1990).

10. T. Inami and C.S. Lim, Prog. Theor. Phys. 65, 297 (1981).

11. J.S. Hagelin and L.S. Littenberg, Prog. Part. Nucl. Phys. 23, 1 (1989), Progress in Nuclear and Particle Physics, September 1989.

12. M. Kobayashi and T. Maskawa, Prog. Theor. Phys. 49, 652 (1973).

13. L. Wolfenstein, Phys. Rev. Lett. 51,1945 (1983).

14. J.S. Haggerty, *Proceedings of the 1990 Snowmass Summer Study*, p. 275.

15. A. Buras and M. Harlander, *Review outline on Heavy Flavors*, ed. A. Buras and M. Lindner, World Scientific, Singapore (1992).

16. G.R. Harris and J.L. Rosner, Phys. Rev. **D 45**, 946 (1992).

17. M. Atiya et al., BNL preprint # 43468, submitted to Phys. Rev. Lett.

18. M. Atiya et al., BNL preprint # 48091, submitted to Phys. Rev. Lett.

19. A. Schwartz, *Fourth Conference on the Intersections between* Particle *and Nuclear Physics*, Tuscon, Arizona, AIP Conference Proceedings No 243, edu., W.T.H. Van Oers (AIP, New York), p. 609.

20. C. Mathiazhagen et al., Phys. Rev. Lett. 63, 2185 (1989).

21. L.M. Sehgal, Phys. Rev. 183, 1511 (1969); B.R. Martin, E. de Rafael, and J. Smith, Phys. Rev. D2, 179 (1970).

22. M.K. Gaillard and B.W. Lee, Phys. Rev. D10, 897 (1974).

23. G. Ecker, A. Pick and E. de Rafael, Nucl. Phys. B291, 692 (1987).

24. P. Bloch et al., Phys. Lett. 56B, 201 (1975).

25. M.E. Zeller, *Rare Decay Symposium*, Vancouver Canada, p. 138 (1988).

26. C. Alliegro et al., Phys. Rev. Lett. 68, 278 (1992).

27. J. Fischer et al., Phys. Lett. 73B, 364 (1978).

28. J.S. Frank et al., Phys. Rev. D28, 423 (1983).

29. K.E. Ohl et al., Phys. Rev. Lett. 64, 2755 (1990).

30. A.S. Carroll et al., Phys. Rev. Lett. 44, 525 (1980).

31. F.J. Gilman and M.B. Wise, Phys. Rev. D21, 3150 (1980).

32. C.O. Dib, I. Dunietz, and F.J. Gilman, Phys. Lett., B218, 487 (1989); C.O. Dib, I. Dunietz, and F.J. Gilman, SLAC preprint, SLAC-PUB-4818, December 1988.

33. L.S. Littenberg, *Proceedings of the Workshop on CP Violation at KAON Factory*, ed. J.N. Ng, p. 19 (1988).

34. W.M. Morse et al., Phys. Rev. D45, 36 (1992).

35. K.E. Ohl et al., Phys. Rev. Lett. 65, 1407 (1990).

36. P.D. Meyers, Moriond talk, March 1989.

37. M.S. Atiya et al., Phys. Rev. Lett. 63, 2177 (1989).

38. L. Littenberg, *Proceedings of the KEK Workshop on Rare Kaon Decay Physics*, Ed. T. Shinkawa, S Sugimoto. Also references within.